Research Article | Vol. 25, No. 20 | 2 Oct 2017 | OPTICS EXPRESS 24650
Optics EXPRESS

Characterization of a FBG sensor interrogation system based on a mode-locked laser scheme

JAVIER MADRIGAL,[1,*] FRANCISCO JAVIER FRAILE-PELÁEZ,[2] DI ZHENG,[1,3] DAVID BARRERA,[1] AND SALVADOR SALES[1]

[1]*Photonics Research Labs, ITEAM research institute, Universitat Politècnica de València, Camino de Vera, s/n, 46022 Valencia, Spain*
[2]*Dept. Teoría de la Señal y Comunicaciones, Universidad de Vigo, ETSI Telecomunicación, Campus Universitario, 36310 Vigo (Pontevedra), Spain*
[3] *Center for Information Photonics & Communications, School of Information Science & Technology, Southwest Jiaotong University, Chengdu, 610031, China*
jamadmad@iteam.upv.es

Abstract: This paper is focused on the characterization of a fiber Bragg grating (FBG) sensor interrogation system based on a fiber ring laser with a semiconductor optical amplifier as the gain medium, and an in-loop electro-optical modulator. This system operates as a switchable active (pulsed) mode-locked laser. The operation principle of the system is explained theoretically and validated experimentally. The ability of the system to interrogate an array of different FBGs in wavelength and spatial domain is demonstrated. Simultaneously, the influence of several important parameters on the performance of the interrogation technique has been investigated. Specifically, the effects of the bandwidth and the reflectivity of the FBGs, the SOA gain, and the depth of the intensity modulation have been addressed.

OCIS codes: (060.3735) Fiber Bragg gratings; (060.2370) Fiber optics sensors; (230.1480) Bragg reflectors;

References and links

1. A. D. Kersey, M. A. Davis, H. J. Patrick, M. LeBlanc, K. P. Koo, C. G. Askins, M. A. Putnam, and E. J. Friebele, "Fiber Grating Sensors," J. Lightwave Technol. **15**(8), 1442–1463 (1997).
2. A. D. Kersey and W. W. Morey, "Multiplexed Bragg grating fibre-laser strain sensor system with mode-locked interrogation," Electron. Lett. **29**(1), 112–114 (1993).
3. D. Chen, C. Shu, and S. He, "Multiple fiber Bragg grating interrogation based on a spectrum-limited Fourier domain mode-locking fiber laser," Opt. Lett. **33**(13), 1395–1397 (2008).
4. R. Huber, M. Wojtkowski, and J. G. Fujimoto, "Fourier Domain Mode Locking (FDML): A new laser operating regime and applications for optical coherence tomography," Opt. Express **14**(8), 3225–3237 (2006).
5. H. Ahmad, H. C. Ooi, A. H. Sulaiman, K. Thambiratnam, M. Z. Zulkifli, and S. W. Harun, "SOA based fiber ring laser with Fiber Bragg Grating," Microw. Opt. Technol. Lett. **50**(12), 3101–3103 (2008).
6. A. E. Siegman, *Lasers* (University Science Books, 1986), Chap. 27.
7. A. Yariv and P. Yeh, *Photonics: Optical Electronics in Modern Communications* (Oxford University Press, 2007), Chap. 16.
8. H. C. Ooi, H. Ahmad, A. H. Sulaiman, K. Thambiratnam, and S. W. Harun, "High-power single-wavelength SOA-based fiber-ring laser with an optical modulator," Laser Phys. **18**(11), 1349–1352 (2008).
9. A. Weiner, *Ultrafast Optics* (Wiley Publishing, 2009), Chap. 2.
10. R. I. Laming, S. Barcelos, W. H. Loh, M. N. Zervas, and M. J. Cole, "Moving fibre/phase mask-scanning beam technique for enhanced flexibility in producing fibre gratings with uniform phase mask," Electron. Lett. **31**(17), 1488–1490 (1995).

1. Introduction

Optical fiber sensors play a pivotal role in several domains such as structural health monitoring, industrial processes and aerospace industry, due to their superior properties over conventional sensors: small dimensions, immunity to electromagnetic interferences, low attenuation, negligible ignition risk, chemically inert character, and harsh environmental conditions resistance. Fiber Bragg Gratings (FBGs) devices are widely used for optical

#303662 https://doi.org/10.1364/OE.25.024650
Journal © 2017 Received 31 Jul 2017; accepted 19 Sep 2017; published 27 Sep 2017

Optics EXPRESS

sensing, and the capability of multiplexing several FBGs in the same fiber is of great interest because it allows for multipoint measurements and reduces the number of sources and detection systems, implying a cost reduction.

A key aspect of optical sensing is the interrogation system. Wavelength-division multiplexing and spatial-division multiplexing are the two main techniques to interrogate multiplexed FBGs [1]. For interrogation purposes, tunable lasers are generally preferred to broadband sources in order to obtain a better signal-to-noise ratio. A characteristic common to most of the schemes proposed in the literature, however, is that they cannot determine the spatial position of the FBGs. In this regard, an initial proposal to determine the spatial positions of the FBGs, based on mode-locked lasers, was developed in [2]. More recently [3], the problem was approached by making use of the so-called Fourier domain mode-locking fiber laser (as opposed to the conventional pulsed mode-locked laser). The structure involves employing a Fabry-Perot tunable filter (FPTF) driven by an electric signal. Although this alternative technique, conceived originally for optical coherent tomography applications [4] and later applied to grating interrogation, has several disadvantages, in practice the FPTF has mechanical parts that can induce stability problems in extreme environments like the aerospace applications. Furthermore, the resolution is fundamentally limited by the slow tuning speed of the FPTF.

To overcome the drawbacks associated to the presence of a FPTF, we present a scheme based on a fiber ring laser with a semiconductor optical amplifier (SOA) as the gain medium, and an in-loop electro-optical modulator instead of a FPTF. This device operates as a switchable active (pulsed) mode-locked laser. In addition to having no mechanical parts, electro-optic modulators offer a bandwidth which is several orders of magnitude higher than the bandwidth allowed by the FPTF, with the result that the spatial resolution is improved by several orders of magnitude.

Section 2 explains the operation principle of the proposed interrogation system for a set of M FBGs arranged in series. Section 3 describes the experimental setup used to validate the interrogation system. The experimental results corroborating the principle of operation are presented next, followed by an analysis of the main characteristics and limitations of the proposed interrogation scheme, and the influence of several key parameters on its performance. Finally, Section 4 summarizes the conclusions obtained.

2. Operation principle

Figure 1 depicts the scheme of the proposed interrogation system. A laser cavity is implemented by means of a semiconductor optical amplifier (SOA) placed within a fiber ring which also includes an electro-optical modulator (EOM) to modulate the intensity of the light, and several FBGs working in reflection mode. The latter are intended to be individually selected, as we will see, and they are incorporated into the cavity optical path through an optical circulator. Optical isolators are adopted to keep the cavity unidirectional and a polarization controller is used to maximize the modulation efficiency.

Referring to Fig. 1, we see that if all the gratings but FBG#1 are removed and the EOM is switched off, the structure corresponds to a standard fiber ring-laser with an in-cavity bandpass filter which restricts the possible lasing frequencies to those inside its bandwidth, much narrower than that of the SOA [5]. The unstructured oscillating modes can be locked by actively modulating the losses with the EOM if the radio-frequency (RF) modulating frequency matches the frequency mode-spacing of the cavity, in the simplest case, or one of its harmonics. The device then operates as an active mode-locked laser yielding a pulsed output with a repetition rate equal to the RF frequency or a multiple of it [6, 7]. Using a SOA as the amplifying medium and one FBG as a narrow-band filter, the continuous (CW) and modulated operation of a similar structure was experimentally studied in [8] aiming to obtain a high-power, low side-mode suppression ratio (SMSR) laser.

Optics EXPRESS

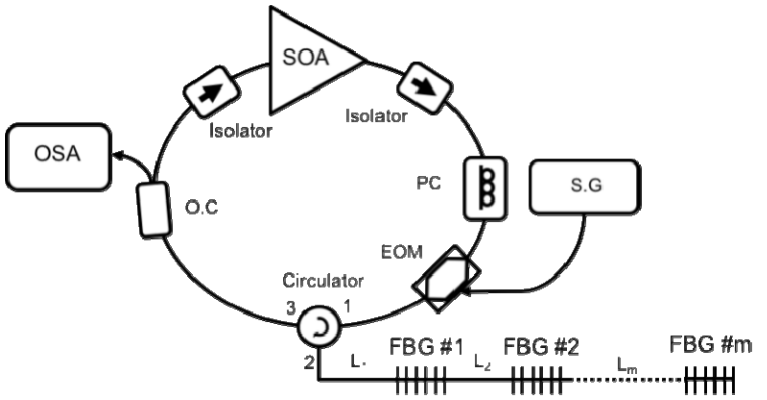

Fig. 1. Schematic of the proposed interrogation system. S.G (signal generator); EOM (electrooptic modulator); O.C (optical coupler); OSA (optical spectrum analyzer); SOA (semiconductor optical amplifier); FBG#1 (1st Fiber Bragg Grating); FBG#2 (2nd FBG); FBG#m (m^{th} FBG); $L_{1\ldots m}$ (lengths from the circulator to each FBG).

The SOA is a wide-band amplifier which covers all the bandwidths of the M FBGs, centered at $\lambda_1, \lambda_2, \ldots, \lambda_m$, respectively. The round-trip transit time for the light reflected by the m-th FBG, is given by $T_m = (L_0 + 2L_m)/v_g$ where L_0 is the fixed fiber length corresponding to the length of the ring and L_m is the fiber length from the circulator to the m-th FBG, and v_g is the group velocity, assuming it is the same along the entire optical path. Therefore, the mode spacing for the resonating frequencies of the m-th cavity is given by:

$$\Delta f_{\mathrm{cav},m} = \frac{v_g}{L_0 + 2L_m}. \tag{1}$$

Mode-locking can thus be accomplished by choosing the RF frequency to be $f_m^{(k)} = k\Delta f_{\mathrm{cav},m}$, where k is a positive integer. Hereafter, we will always chose the fundamental cavity frequency, $f_m^{(1)} = \Delta f_{\mathrm{cav},m} \equiv f_m$, dropping the unnecessary superindex $^{(1)}$.

In the absence of modulation, since no FBG is shadowed by any other and the wavelength separation between adjacent gratings is moderate (~0.5 nm – 2 nm), lasing should start almost simultaneously at all allowed λ_m, as soon as a sufficient level of SOA gain is reached. Note that each of the "M lines" is really composed of numerous oscillating frequencies around the nominal wavelength λ_m. Now, if an RF tone at the specific frequency f_n is applied to the EOM, the lasing line at λ_n will become mode-locked, whereas the rest of the lines will still contain free-running modes (the positions L_m of the FBGs are chosen so as to avoid harmonic relations among the frequencies f_m). If modulation is then switched on at any particular cavity frequency f_n, all lines will disappear except that corresponding to λ_n, which will remain essentially the same. This is because the intensity modulation induces losses. Since all the λ_m with free-running modes were kept lasing only slightly above their threshold, a small increase of the average loss can easily pull them out of oscillation. The case of λ_n is different, however, due to the mode-locking of the modes of the n-th cavity. The amplitude modulation affects each and every mode inducing two, right and left, sidebands which coincide exactly with the adjacent oscillating modes because of the condition $f_n = \Delta f_{\mathrm{cav},\,n}$ (which is not the case for the free-running modes of the other λ_m lines). This causes a coherent redistribution of the energy among all the modes, which can even reach some previously under-threshold frequencies located at both ends of the FBG passband. These are fed from the central modes, where the gain now exceeds the losses, and locked to the whole oscillating frequency set [9].

Optics EXPRESS

However, if the SOA gain is further increased, it will soon compensate for the losses of the free running modes comprising all the other λ_m lines, $m \neq n$, which will thus oscillate again, so that discriminating the mode-locked cavity will no longer be straightforward.

3. Experimental measurements

To validate the proposed interrogation scheme, we fabricated three FBGs that were placed in series following the scheme in Fig. 1. A 99:1 optical coupler was used to tap the output of the ring laser while minimizing the losses in the loop, and two optical isolator were inserted at both ends of the SOA in order to reject the possible reflections generated inside the loop. A lithium niobate EOM with a 20 GHz bandwidth was employed for the RF modulation.

The FBGs were fabricated in our laboratory in a standard single-mode fiber (SMF) which was previously hydrogen-loaded at 20 bar pressure for two weeks at ambient temperature in order to increase its photo-sensitivity. The FBG writing process was done using a 244 nm CW frequency-double argon-ion laser with the moving fibre/phase mask-scanning beam technique [10]. Figure 2 shows the measured FBG spectra.

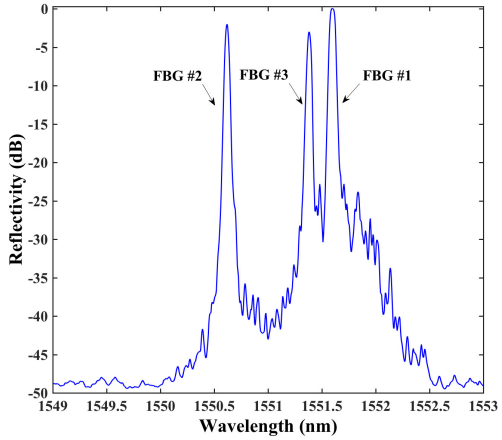

Fig. 2. Spectra of the FBGs under test.

We chose unequal FBGs in order to show the potential of the proposed interrogation technique. Namely, FBG#1 has a reflectivity of 99.9% and a bandwidth of 56.2 pm, FBG#2 has a reflectivity of 63.5% and a bandwidth of 38.7 pm, and FBG#3 has a reflectivity of 49.5% and a bandwidth of 35.1 pm. The total lengths of the loops are determined by the lengths of the different fiber sections, which are as follows: L_0 = 19.13 m, L_1 = 2.75 m, L_2 = 5.64 m, and L_3 = 9.95 m. According to Eq. (1), the resonating frequencies are f_1 = 8.4 MHz, f_2 = 6.8 MHz, and f_3 = 5.3 MHz.

Initially, we modulated the EOM with a sinusoidal signal at different frequencies. Figure 3 shows the spectra of the resonant peaks. As it was expected, when the frequency applied to the EOM differs from the cavity resonant frequencies, no peaks appear or they have a very low power; but when the frequency matches one of the resonant frequencies, a significant peak at the corresponding FBG wavelength emerges. A signal-to-noise ratio (SNR) better than 25 dB was obtained.

Optics EXPRESS

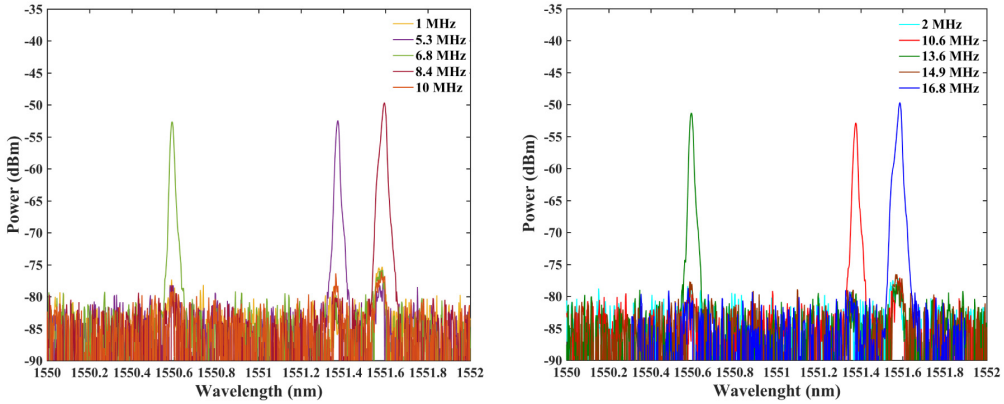

Fig. 3. Ring laser output spectra at different EOM modulating RF tones from 1 to 16.8 MHz.

Figure 3 shows the optical spectra corresponding to the RF frequencies f_1 (left) and f_2 (right). The resolution of the OSA does not allow to observe the substructure of each optical line. In order to check that the selected cavity behaves as a mode-locked laser, the loop-circulating signal was photodetected and its electrical spectrum measured. Figure 4 shows the spectrum obtained when one of the RF resonant frequencies (5.3 MHz) is applied to the EOM. The spectrum is clean and reveals the presence of the fundamental peak frequency at 5.3 MHz and its harmonics, which clearly indicates the periodic nature of the pulsed optical signal. This evidences that the targeted cavity does indeed operate under the expected mode-locking regime, while the others do not.

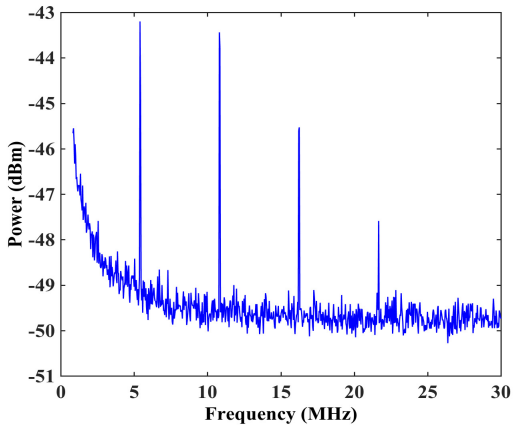

Fig. 4. Electrical spectrum of the photo-detected signal when the modulation frequency is 5.3 MHz.

We have investigated the influence of several important parameters on the performance of the interrogation technique. Specifically, we have addressed the effects of the bandwidth and the reflectivity of the FBGs, the SOA gain, and the depth of the intensity modulation. Figure 5 shows two recorded spectrograms, corresponding to two different values of the SOA injection current. The optical power, represented by the color scale, is given as the optical wavelength and the modulation frequency are swept within the ranges shown. The EOM employed was a Mach-Zenhder modulator (MZM) with a quadrature voltage V_π = 6 V, to which a sinusoidal signal was applied with a peak-to-peak voltage V_{pp} = 5 V.

Optics EXPRESS

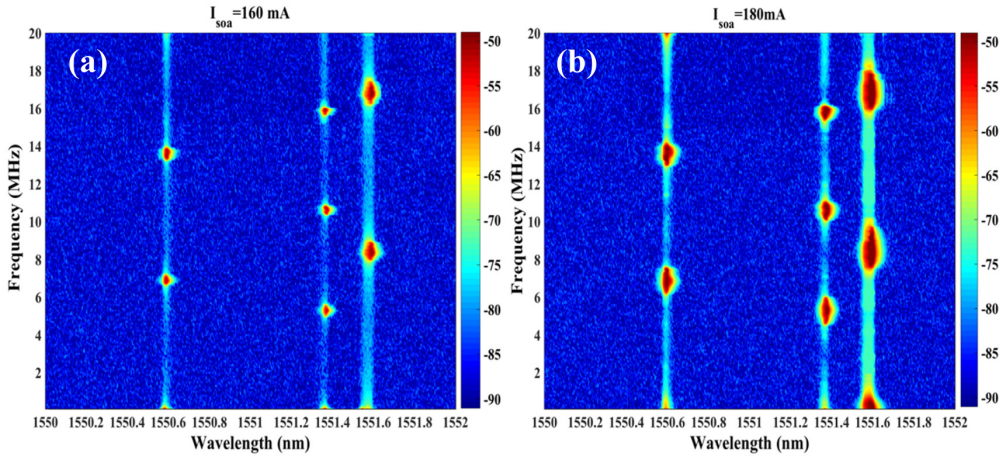

Fig. 5. Spectrogram at different SOA injection currents 160 mA (a) and180 mA (b).

Figure 5 consistently shows the peak of each FBG appearing whenever the RF modulation frequency matches the corresponding cavity resonant frequency, and this actually occurs within a small range around the nominal values of frequency and wavelength. We will first focus on the effect of the FBG. The spectrograms reveal that the maximum allowable RF detuning before the output power quickly drops, is greater for FBG#1 than for the other, weaker, FBGs. This can be understood in terms of the extent of the set of oscillating frequencies. When the RF frequency deviates slightly from the cavity resonance frequency, the coherent locking of the modes gradually tends to vanish and modulation-induced losses grow. If the FBG with high reflectivity has a broad spectral range, more oscillating modes exist and a larger RF detuning is necessary for the induces losses to extinguish the laser oscillation.

Note that the frequency sweeping range is large enough to detect some harmonic mode-locking, if it occurs. Indeed, even if we have not focused on this possibility, we find that not only the peaks at the frequencies $f_m \equiv f_m^{(1)}$ (m = 1, 2, 3) appear in Fig. 5, but also all the second harmonics $f_m^{(2)}$, and even one third harmonic, $f_3^{(3)}$.

The influence of the SOA gain is illustrated by comparing Figs. 5a and 5b, which correspond to two different values of the SOA injection current. As expected, a lower SOA gain yields lower SNR but higher spatial accuracy because a lower gain results in a smaller detuning required for the output power of each FBG resonance to drop. (see Section 2). The best spatial accuracy is obtained when the ring cavity laser is operating closest to its threshold (Fig. 5a). The detuning from the resonant frequency at FBG#3 (Fig. 5a) is around 250 kHz, which implies a spatial accuracy of 45 cm.

If the modulation depth at the EOM is increased by choosing V_{pp} = 8 V, which exceeds V_π, new resonant frequencies may appear at submultiples of the initial resonances due to over-modulation process, as can be observed in Fig. 6. Thus, if we focus on the strongest FBG (FBG#1), we see that some small peaks appear at several unexpected frequencies around 2.8 MHz, 4.2 MHz and 5.6 MHz, along with others. Indeed, for a modulation frequency of 2.8 MHz, the 3rd harmonic corresponds to 8.4 MHz and matches the resonance frequency of the FBG#1, causing the appearance of the peak at this frequency. Similarly, 8.4 MHz, which is the 2nd harmonic of 4.2 MHz, and 16.8 MHz, which is the 3rd harmonic of 5.6 MHz, respectively match the resonance frequency of FBG#1 and its first overtone.

Optics EXPRESS

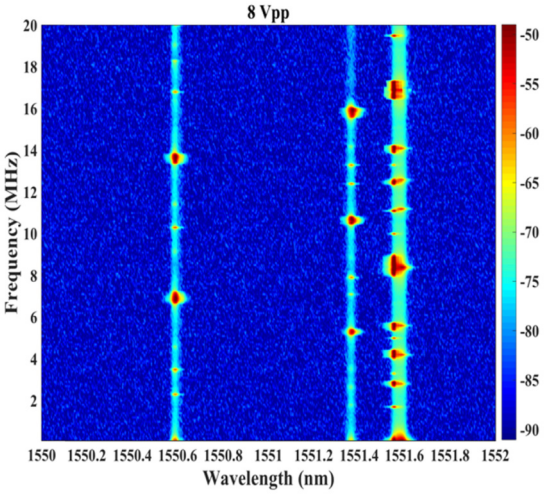

Fig. 6. Spectrogram when the Vpp is 8V, that it is higher than the V_π of the MZM.

Finally, we have verified the behavior of the proposed scheme when one of the FBGs is submitted to a change in temperature (FBG#3). Figure 7 shows that the interrogation system can still determine the spatial position when the FBG is wavelength value is shifted by temperature changes. Figure 7a shows some of the spectra of FBG#3 when it is heated/cooled from 30 °C to –20 °C. Figure 7b shows a linear behavior, as it corresponds to an FBG sensor with a temperature coefficient of 10 pm/°C.

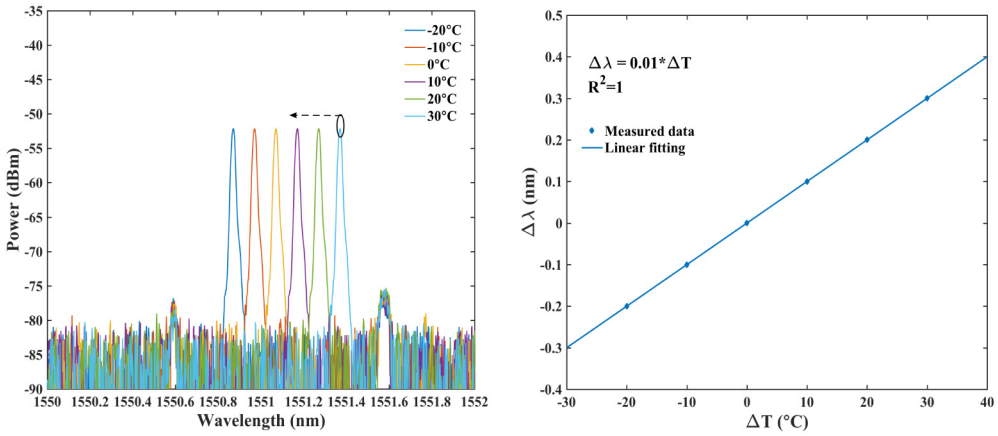

Fig. 7. FBG#3 spectra for different temperatures (left) and wavelength shift vs temperature shift (right).

4. Conclusions

We have presented a FBG interrogation system based on a fiber ring laser with a semiconductor optical amplifier as the gain medium, and an in-loop electro-optical modulator instead of a FPTF which allows to overcome the drawbacks derived from the use of mechanical parts, while, on the other hand, increases the spatial accuracy by several orders of magnitude. By sequentially setting the modulation frequency to each value of the FBG resonance frequencies, we can interrogate the spatial positions of the FBGs placed in series along the fiber. We can thus interrogate different FBGs using the same wavelength without any response overlapping, provided their separation is larger than the spatial resolution.

Optics EXPRESS

Additionally, the selected FBG can be interrogated in the wavelength domain through measurement of the output optical spectrum.

The operation principle of the interrogation system proposed has been explained theoretically and tested experimentally in the laboratory, where an array of three different FBGs placed in series was used to characterize the system.

The role of several important parameters on the performance of the interrogation technique has been investigated. We have addressed the effect of the characteristics of the FBGs and the SOA gain on the spatial accuracy. The reflectivity and the bandwidth of the FBG influence the spatial accuracy, with the result that a weaker FBG requires a smaller detuning range to extinguish the output power from the FBG resonance, thus improving the spatial accuracy. A lower SOA injection current also yields better spatial resolution.

As for the effect of the RF modulator, we have seen that the employment of a reasonable large modulation depths is feasible, but a voltage excursion V_{pp} roughly higher than the value V_{π} of the EOM may cause resonant peaks to appear at unexpected frequencies. Even if this are easily identified and isolated in our case, it might become cumbersome to handle them as the number of FBGs increases.

Finally, to validate the proposed interrogation system, we have heated/cooled an FBG sensor with a temperature coefficient of 10 pm/°C, and have demonstrated that the interrogation system can still determine the spatial position when the FBG is wavelength shifted due to temperature changes.

While there are interrogation schemes with better performance than our design when the focus is put on the sensitivity to the magnitude of the event (temperature, strain) or its frequency response (vibration), our proposed interrogator system allows to multiplex a large number of multiplexing reflective sensors and also provides excellent spatial resolution for applications where it is important to localize the presence of hot spots or some any other event that is placed at an unknown position. Compared to previous interrogation methods concerned with the spatial resolution, our scheme yields a remarkable SNR of almost 30 dB, and dispenses with the mechanical elements employed in previous configurations, which are subject to sweep velocity constrains.

Funding

This work has been partially supported by the Spanish MINECO through project TEC2014-60378-C2-1-R MEMES; the Generalitat Valenciana (APOSTD/2016/015), Sistema Nacional de Garantía Juvenil grant PEJ-2014-A-75865 (Promoción de Empleo Joven e Implantación de la Garantía Juvenil 2014, MINECO); the Galician Regional Government under project GRC2015/018; the support of FINESSE the European Union's Horizon 2020 research and innovation programme under the Marie Sklodowska - Curie Action grant agreement n° 722509; the National Natural Science Foundation of China (61405166) and the China Scholarship Council.